2018 5th International Workshop on Compressed Sensing applied to Radar, Multimodal Sensing, and Imaging (CoSeRa)

Resolution Analysis of Compressive Data Acquisition

Radmila Pribić

Sensors Advanced Developments
Thales Nederland Delft
Delft, The Netherlands

***Abstract*— A stochastic approach to resolution is explored by using information distances computed from the geometry of data models which is characterized by the Fisher information. Taking information distances into account is crucial in compressive data acquisition typical for compressive sensing (CS). Based on this information-geometry approach, we assess the stochastic resolution bounds from data models with typical compressive measurements and with the Nyquist-sampled measurements as the reference. Such resolution bounds are also compared with actual resolution obtained from sparse signal processing that is nowadays a major part of the back end of a radar system with CS. The resolution analysis demonstrates that only with a compressive data acquisition scheme of random masking (starting directly at reception, with no receiver noise yet), compressive measurements can perform as good as Nyquist-sampled measurements.**

***Keywords*— compressive measurements; stochastic resolution; information geometry; array processing; radar;**

I. Introduction

Compressive sensing (CS) is a recent paradigm in sensing that works with a reduced number of measurements for a comparable sensing result. This is possible because CS is optimized to available information in measurements rather than to the sensing bandwidth only. The optimization is based on two conditions: sparsity of sensing results and the sensing incoherence (e.g. [1]). In a CS sensor, sparse signal processing (SSP) is crucial in the back end, while its front end facilitates compressive data acquisition. The ultimate goal of CS is a CS sensor which is simpler and still performs at least as good as, or even better than, existing sensors.

Compressive data acquisition and also a whole CS sensor are regularly believed to be less complicated (and even less costly) while performing satisfactorily. However, the performance and overall processing gain in CS are becoming additionally important and delicate due to fewer measurements (e.g. [2]-[3]). As we focus on a CS sensor as a whole, we check how fewer measurements from the compressive data acquisition affect the performance of SSP in the back end. Therefore, we assess the resolution potential of different compressive data acquisition schemes (given the same input signal). We show that with the scheme applied directly at reception (e.g. [4]-[5]), a CS sensor can be simpler and still perform as good as existing sensors.

Resolution is primarily described by the minimum distance between two objects that a sensor can resolve (e.g. [6]). Stochastic resolution has been introduced in [7] by including the Cramér-Rao bound (CRB). This stochastic approach was extended with the probability of resolution at a given separation and signal-to-noise ratio (SNR) obtained via an asymptotic generalized likelihood ratio (GLR) test based on Euclidean distances ([8]). Information distances and resolution have also been explored with an arbitrary test ([9]). Information geometry (IG, [9]-[11]) and CS ([1] and [12]-[13]) have the potential to contribute to the completeness of the stochastic approach, due to their focus on information content ([3], [5] and [14]-[17]). In [16]-[17], the Fisher-Rao information distance is recognized in the asymptotic GLR. In [3], different information distances are linked to the LR and applied to Nyquist and sub-Nyquist random measurements.

In this paper, the stochastic resolution analysis from [3] is focused on different compressive data acquisition schemes.

A. Related Work

During substantial CS research in the decade starting in 2005 (e.g. [1] and [12]-[13]), no complete guarantees of CS-sensor resolution performance were developed yet. In particular, the analysis of compressive data acquisition was lacking.

Stochastic resolution limits were studied (e.g. [7] and [8]) but without IG or CS. Information resolution was studied (e.g. [9]) but not via (G)LRT nor linked to the CS-radar resolution. The stochastic resolution was analyzed via (G)LR and compared to the SSP resolution in [3] and [16]-[17].

In addition, in [3], fewer random measurements are also used. In this paper, the resolution analysis is extended and committed to typical compressive data acquisition schemes.

B. Outline and Main Contributions

In Section II, relevant data acquisition schemes are presented starting with the Nyquist scheme as the reference, followed by two typical sub-Nyquist schemes from [5]. In Section III, stochastic resolution analysis [3] is applied to the data acquisition schemes. In Section IV, numerical results supporting the analysis are presented. In the end, conclusions are drawn and future work indicated.

Our main contribution is the resolution analysis of typical data acquisition schemes in CS. Furthermore, we compare compressive data acquisition with a corresponding existing scheme as the reference. Finally, when looking at a CS sensor as a whole, we reveal that a CS sensor with certain compressive data acquisition can be less involved and still perform as good as existing sensors.

II. Compressive Data Acquisition

Compressive data acquisition may change processing gain and sensing performance (e.g. [2]-[3]). We are interested in acquisition schemes with Nyquist-sampled data as the reference, and with typical sub-Nyquist data compressed before and at reception (which remain Gaussian-distributed).

In an array of size N, raw complex-valued measurements gathered in a vector $\boldsymbol{y} \in \mathbb{C}^N$ of an input (true) signal $\boldsymbol{s} \in \mathbb{C}^K$ from K point targets can be modelled as (e.g. [18]):

$$\boldsymbol{y} = \sum_{k=1}^{K} s_k e^{j\boldsymbol{\beta}\theta_k} + \boldsymbol{z} = \sum_{k=1}^{K} s_k \boldsymbol{a}(\theta_k) + \boldsymbol{z}, \qquad (1)$$

where s_k is the kth-target echo in $\boldsymbol{s}$, $\boldsymbol{\beta} \in \mathbb{R}^N$ is an observation vector (centered, i.e. $\sum_n \beta_n = 0$), θ_k is an unknown, $\boldsymbol{z}$ is a (complex Gaussian) receiver-noise vector of i.i.d. elements with zero mean and equal variances γ, $\boldsymbol{z} \sim CN(\boldsymbol{0}, \gamma \boldsymbol{I}_N)$ and $\boldsymbol{a}(\theta)$ is a sensing vector with norm $\sqrt{N}$, $\boldsymbol{a}(\theta) = e^{j\boldsymbol{\beta}\theta}$. In a spatial array, β_n and θ_k would yield the antenna-element position and unknown angle, respectively.

For the sake of an information distance between $CN(\boldsymbol{\mu}(\theta), \gamma\boldsymbol{I}_N)$ and $CN(\boldsymbol{\mu}(\theta+\delta\theta), \gamma\boldsymbol{I}_N)$ and its link to resolution ([3]), we investigate $\boldsymbol{s}$ which contains a single nonrandom component. The reference Nyquist-sampled (NS) data $\boldsymbol{y} \in \mathbb{C}^N$, $\boldsymbol{y} \sim CN(\boldsymbol{\mu}(\theta), \gamma\boldsymbol{I}_N)$, can be written as:

$$\boldsymbol{y} = \boldsymbol{a}(\theta)s + \boldsymbol{z} = \boldsymbol{\mu}(\theta) + \boldsymbol{z} \equiv \boldsymbol{\mu} + \boldsymbol{z} \qquad (2)$$

where $\boldsymbol{a}(\theta) \in \mathbb{C}^{N\times 1}$ is a sensing vector belonging to the nonzero response s at θ and $\boldsymbol{z}$ is as before, $\boldsymbol{z} \sim CN(\boldsymbol{0}, \gamma\boldsymbol{I}_N)$. The complex-valued target echo s is assumed to have constant nonrandom amplitude $|s|$ (so-called SW0, [19]). The related signal-to-noise ratio (SNR) is equal to $|s|^2/\gamma$.

We investigate compressive data acquisition with two sub-Nyquist data models containing the Gaussian noise. First we look at compression before reception, namely at sparse sensing (SS, e.g. [20]). Further, we look at random masking (RM, e.g. [4]-[5]) which enables the compression directly at reception where receiver noise can be ignored.

In the SS scheme, the corresponding model of the compressed data $\boldsymbol{y}_{\mathrm{SS}} \in \mathbb{C}^M$, $M < N$, can be written as follows:

$$\boldsymbol{y}_{\mathrm{SS}} = \boldsymbol{B}_{\mathrm{SS}}\boldsymbol{y} = \boldsymbol{B}_{\mathrm{SS}}\boldsymbol{\mu} + \boldsymbol{B}_{\mathrm{SS}}\boldsymbol{z} = \boldsymbol{\mu}_{\mathrm{SS}} + \boldsymbol{z}_{\mathrm{SS}} \qquad (3)$$

where the compression matrix $\boldsymbol{B}_{\mathrm{SS}}$ has M ones (chosen in a multi-coset manner, e.g. [19]) one on every row and zeros elsewhere. Accordingly, $\boldsymbol{y}_{\mathrm{SS}}$, $\boldsymbol{\mu}_{\mathrm{SS}}$ and $\boldsymbol{z}_{\mathrm{SS}}$ contain the corresponding M elements from $\boldsymbol{y}$, $\boldsymbol{\mu}$ and $\boldsymbol{z}$, respectively. Thus, there are M outputs, each output having the noise as in the reference case, $\boldsymbol{z}_{\mathrm{SS}} \sim CN(\boldsymbol{0}, \gamma\boldsymbol{I}_M)$. From a single realization of $\boldsymbol{B}_{\mathrm{SS}}$, we can assume $\boldsymbol{y}_{\mathrm{SS}} \sim CN(\boldsymbol{\mu}_{\mathrm{SS}}, \gamma\boldsymbol{I}_M)$.

In the RM scheme, the related model of the compressed data $\boldsymbol{y}_{\mathrm{RM}} \in \mathbb{C}^M$, $M < N$, can be written as follows:

$$\boldsymbol{y}_{\mathrm{RM}} = \boldsymbol{B}_{\mathrm{RM}}\boldsymbol{\mu} + \boldsymbol{z}_{\mathrm{RM}} = \boldsymbol{\mu}_{\mathrm{RM}} + \boldsymbol{z}_{\mathrm{RM}} \qquad (4)$$

where the compression matrix $\boldsymbol{B}_{\mathrm{RM}}$ is a full random matrix. We investigate a practical $\boldsymbol{B}_{\mathrm{RM}}$ which contains uniformly-distributed phase shifts. Its mn–th element $b_{\mathrm{RM},mn}$ equals $\exp(j\varphi_{mn})/\sqrt{M}$ where $\varphi_{mn} \sim U(0,2\pi)$. In RM, $\boldsymbol{B}_{\mathrm{RM}}$ affects only the signal as it works at reception without any receiver noise yet. After reception there are M outputs whose receiver noise is equivalent to the SS case, i.e. $\boldsymbol{z}_{\mathrm{RM}} \sim CN(\boldsymbol{0}, \gamma\boldsymbol{I}_M)$, and $\boldsymbol{y}_{\mathrm{RM}} \sim CN(\boldsymbol{\mu}_{\mathrm{RM}}, \gamma\boldsymbol{I}_M)$ from a single realization of $\boldsymbol{B}_{\mathrm{RM}}$.

In CS, the solution for the unknown $\boldsymbol{s}$ from data models (1)-(4) is sought by applying the model: $\boldsymbol{y}_{\mathrm{c}} = \boldsymbol{A}_{\mathrm{c}}\boldsymbol{x} + \boldsymbol{z}_{\mathrm{c}}$ where $\boldsymbol{A}_{\mathrm{c}}$ is the sensing matrix over a discrete grid of size N, $\boldsymbol{A}_{\mathrm{c}} \in \mathbb{C}^{M\times N}$ and $\boldsymbol{x}$ is a sparse vector, $\boldsymbol{x} \in \mathbb{C}^N$. The usual SSP, e.g. LASSO [21], applies as:

$$\boldsymbol{x}_{\mathrm{SSP}} = \arg\min_{\boldsymbol{x}} \|\boldsymbol{y}_{\mathrm{c}} - \boldsymbol{A}_{\mathrm{c}}\boldsymbol{x}\|^2 + \eta\|\boldsymbol{x}\|_1 \qquad (5)$$

where the l_1-norm $\|\boldsymbol{x}\|_1$ promotes sparsity, the l_2-norm $\|\boldsymbol{y}_{\mathrm{c}} - \boldsymbol{A}_{\mathrm{c}}\boldsymbol{x}\|$ minimizes the errors, and a regularization parameter η balances between the two tasks. The parameter η is closely related to the detection threshold (e.g. [24]). An underdetermined system can be solved, $M < N$, because of the sparsity, i.e. only K nonzeros in $\boldsymbol{x}$ (representing the unknown $\boldsymbol{s}$), $K < M < N$, and because of the incoherence of $\boldsymbol{A}_{\mathrm{c}}$ (e.g. [1]). The mutual coherence $\kappa(\boldsymbol{A})$ of a matrix $\boldsymbol{A}$ is an incoherence measure, $\kappa(\boldsymbol{A}) = \max_{i,j,i\neq j} |\boldsymbol{a}_i^{\mathrm{H}}\boldsymbol{a}_j| / \|\boldsymbol{a}_i\|\|\boldsymbol{a}_j\|$ where $\boldsymbol{a}_n$ is the nth column of $\boldsymbol{A}$, $n = 1, .., N$.

In radar processing, a sensing matrix $\boldsymbol{A}$ is intrinsically deterministic and its incoherence is also intrinsically strong because of the physics of radar sensing. In array processing as in (1), the sensing matrix $\boldsymbol{A}_{\mathrm{c}}$ from (5) is often an (I)FFT matrix, i.e. $\kappa(\boldsymbol{A}_{\mathrm{c}}) = 0$ when $M = N$. With a uniform array of size M, the grid cell $\Delta\theta$ is $2\pi/M$ large. Such a cell size is called the Nyquist size. Fewer measurements, i.e. when $M < N$, or a smaller cell $\Delta\theta$ would make $\kappa(\boldsymbol{A}_{\mathrm{c}})$ increase.

III. Stochastic Resolution Analysis

Our resolution analysis is based on distances between two populations that have been studied in information geometry (IG). IG studies manifolds in the parameter space of probability distributions, using the tools of differential geometry (e.g. [10] and [11]). The inner product of two vectors $\boldsymbol{v}$ and $\boldsymbol{w}$ in a Euclidean space: $\langle\boldsymbol{v},\boldsymbol{w}\rangle = \boldsymbol{v}^{\mathrm{H}}\boldsymbol{w}$ is redefined locally as: $\langle\boldsymbol{v},\boldsymbol{w}\rangle = \boldsymbol{v}^{\mathrm{H}}\boldsymbol{G}\boldsymbol{w}$, where $\boldsymbol{G}$ is a crucial metric defined by the Fisher information matrix (FIM) in IG.

In the accuracy analysis, the metric $\boldsymbol{G}(\boldsymbol{\theta})$ is typically applied to the Cramér-Rao bound (CRB) of the mean squared error (MSE) of an unbiased estimator $\hat{\boldsymbol{\theta}}$ of $\boldsymbol{\theta}$, i.e. $\mathrm{MSE}(\hat{\boldsymbol{\theta}}) \geq \mathrm{CRB}(\boldsymbol{\theta}) = [\boldsymbol{G}(\boldsymbol{\theta})]^{-1}$ (e.g. [18]).

In addition, $\boldsymbol{G}(\boldsymbol{\theta})$ is also used for resolution bounds based on information distances between $p(\boldsymbol{y}|\boldsymbol{\theta})$ and $p(\boldsymbol{y}|\boldsymbol{\theta} + d\boldsymbol{\theta})$ when $\boldsymbol{\theta}$ change a bit by $d\boldsymbol{\theta}$ (e.g. [3], [9] and [16]-[17]).

A. *Information Distances*

An information distance $d_{\boldsymbol{\mu}(\theta)}$ between $CN(\boldsymbol{\mu}(\theta), \boldsymbol{\Sigma})$ and $CN(\boldsymbol{\mu}(\theta+\delta\theta), \boldsymbol{\Sigma})$ with the same covariance $\boldsymbol{\Sigma}$, $\boldsymbol{\Sigma} = \gamma\boldsymbol{I}_N$, and different means, $\delta\boldsymbol{\mu} = \boldsymbol{\mu}(\theta+\delta\theta) - \boldsymbol{\mu}(\theta)$, is derived analog to the distance from [10] between $N(\mu,\gamma)$ and $N(\mu+\delta\mu,\gamma)$ on the manifold in $(\mu, \sqrt{\gamma})$. The distance $d_{\boldsymbol{\mu}(\theta)}$ can be given by the Mahalanobis distance (e.g. [22]) as follows:

$$d_{\boldsymbol{\mu}(\theta)} = \sqrt{\delta\boldsymbol{\mu}^H \boldsymbol{G} \delta\boldsymbol{\mu}} = \|\delta\boldsymbol{\mu}\|/\sqrt{\gamma} \ , \quad (6)$$

where $\boldsymbol{G}$ is the inverse of $\boldsymbol{\Sigma}$. We realize that the FIM for the mean $\boldsymbol{\mu}$ also equals $\boldsymbol{G}$ defined as follows (e.g. [23]):

$$\boldsymbol{G} = -\mathrm{E}\left[\frac{\partial^2 \ln p(\boldsymbol{y}|\boldsymbol{\mu}(\theta))}{\partial\boldsymbol{\mu}\partial\boldsymbol{\mu}^H}\right] = \frac{1}{\gamma}\frac{\partial}{\partial\boldsymbol{\mu}^H}\frac{\partial\boldsymbol{\mu}^H\boldsymbol{\mu}}{\partial\boldsymbol{\mu}} = \frac{1}{\gamma}\frac{\partial}{\partial\boldsymbol{\mu}^H}\boldsymbol{\mu}^* = \frac{1}{\gamma}\boldsymbol{I}_N$$

where $\boldsymbol{\mu}^*$ is the complex conjugate of $\boldsymbol{\mu}$, and $\boldsymbol{\mu}^H \equiv \boldsymbol{\mu}^{*T}$.

Next we apply (6) to the three acquisition schemes: NS, SS and RM from (2), (3) and (4), respectively.

The distance $d_{\boldsymbol{\mu}(\theta),\mathrm{NS}}$ with NS from (2) can be derived as:

$$d_{\boldsymbol{\mu}(\theta),\mathrm{NS}} = \|\delta\boldsymbol{\mu}_{\mathrm{NS}}\|/\sqrt{\gamma} \rightarrow \sqrt{\frac{\mathrm{D}_\beta |s|^2}{\gamma}\left(1 - \frac{\sin \mathrm{D}_\beta \delta\theta/2}{\mathrm{D}_\beta \delta\theta/2}\right)} \quad (7)$$

where D_β is the array (aperture) size, $\mathrm{D}_\beta = \max_n \beta_n - \min_n \beta_n$. The closed form is obtained when the observation variable β is treated as continuous in the norm $\|\delta\boldsymbol{\mu}\| \rightarrow \|\delta\mu(\beta,\theta)\|$, $-\mathrm{D}_\beta/2 \leq \beta \leq \mathrm{D}_\beta/2$. The continuous domain enables the ultimate reference before any sampling (as a subject of further work). Note that there appears a complete set of parameters affecting the resolution: D_β, SNR and $\delta\theta$.

The distance $d_{\boldsymbol{\mu}(\theta),\mathrm{SS}}$ expected with SS in (3) is given by:

$$d_{\boldsymbol{\mu}(\theta),\mathrm{NS}} = \mathrm{E}\left[\frac{\|\delta\boldsymbol{\mu}_{\mathrm{SS}}\|}{\sqrt{\gamma}}\right] = E\left[\sqrt{\frac{\delta\boldsymbol{\mu}^{\mathrm{H}}\boldsymbol{B}_{\mathrm{SS}}^{\mathrm{H}}\boldsymbol{B}_{\mathrm{SS}}\boldsymbol{\mu}}{\gamma}}\right] = \sqrt{\frac{M}{N}}\, d_{\boldsymbol{\mu}_{\mathrm{NS}}(\theta)} \quad (8)$$

as $\boldsymbol{B}_{\mathrm{SS}}^{\mathrm{H}}\boldsymbol{B}_{\mathrm{SS}}$ is an NxN diagonal matrix with only M ones on the diagonal and zeros elsewhere, $M < N$.

The distance $d_{\boldsymbol{\mu}(\theta),\mathrm{RM}}$ expected with RM from (4) where $\mathrm{E}[\boldsymbol{B}_{\mathrm{RM}}^{\mathrm{H}}\boldsymbol{B}_{\mathrm{RM}}] = \boldsymbol{I}_N$ is given by:

$$d_{\boldsymbol{\mu}(\theta),\mathrm{RM}} = \mathrm{E}\left[\frac{\|\delta\boldsymbol{\mu}_{\mathrm{RM}}\|}{\sqrt{\gamma}}\right] = E\left[\sqrt{\frac{\delta\boldsymbol{\mu}^{\mathrm{H}}\boldsymbol{B}_{\mathrm{RM}}^{\mathrm{H}}\boldsymbol{B}_{\mathrm{RM}}\boldsymbol{\mu}}{\gamma}}\right] = d_{\boldsymbol{\mu}_{\mathrm{NS}}(\theta)} \quad (9)$$

as $\mathrm{E}\left[b^*_{\mathrm{RM},ml} b_{\mathrm{RM},mk}\right]$ equals 1 when $l = k$, and 0 otherwise.

Hence, RM preserves the information distance from NS while SS makes it decrease proportionally with $\sqrt{M/N}$.

Next we derive the stochastic resolution bounds from the distance $d_{\boldsymbol{\mu}(\theta)}$ in (6) as the probability that two point targets can be resolved at a separation $\delta\theta$ and a particular SNR.

B. *Stochastic Resolution*

In some early work on IG [10], Rao proposed testing the resolution in θ from data $\boldsymbol{y}$ with a hypothesis H_0: $\delta\theta = 0$ and its alternative H_1: $\delta\theta \neq 0$, by using a distance between the data populations $p(\boldsymbol{y}|\theta)$ and $p(\boldsymbol{y}|\theta + \delta\theta)$.

In [3], the equivalent binary hypothesis at the true separation $\delta\theta$ is expressed as follows:

$$\begin{aligned} H_0&: \boldsymbol{y} = 2\boldsymbol{\mu}(\theta) + \boldsymbol{z} = \boldsymbol{y}_0 \\ H_1&: \boldsymbol{y} = \boldsymbol{\mu}(\theta) + \boldsymbol{\mu}(\theta + \delta\theta) + \boldsymbol{z} = \boldsymbol{y}_0 + \delta\boldsymbol{\mu} \end{aligned} \quad . \quad (10)$$

where the data $\boldsymbol{y}$ as in (2)-(4) contain responses from two point targets separated by $\delta\theta$. Consequently, the likelihood ratio (LR), $\mathrm{LR} = p(\boldsymbol{y}|\theta, \theta + \delta\theta)/p(\boldsymbol{y}|\theta)$, is explored. From (10), a test statistic $\ln \mathrm{LR}$ is derived as follows:

$$\ln \mathrm{LR} = (2Re\,\{[\boldsymbol{y} - 2\boldsymbol{\mu}(\theta)]^H \delta\boldsymbol{\mu}\} - \|\delta\boldsymbol{\mu}\|^2)/\gamma \quad (11)$$

whose Gaussian distribution is defined with the distance $d_{\boldsymbol{\mu}(\theta)}$ from (6), $\ln \mathrm{LR} \sim N(\mp d^2_{\boldsymbol{\mu}(\theta)}, 2d^2_{\boldsymbol{\mu}(\theta)})$. Thus, a link is established between a resolution test and an information distance between $CN(\boldsymbol{\mu}(\theta), \boldsymbol{\Sigma})$ and $CN(\boldsymbol{\mu}(\theta + \delta\theta), \boldsymbol{\Sigma})$.

In order to assess the probability of resolution $P_{\mathrm{res},\mu}$, the $\ln \mathrm{LR}$ from (11) is tested with a test statistic $\xi_{\mathrm{LR},\boldsymbol{\mu}(\theta)}$ under H_1, $\xi_{\mathrm{LR},\boldsymbol{\mu}(\theta)} = \ln \mathrm{LR}/2d_{\boldsymbol{\mu}(\theta)} + d_{\boldsymbol{\mu}(\theta)}/2 \sim N(d_{\boldsymbol{\mu}(\theta)}, 1)$, against a threshold ρ obtained under H_0 from the inverse normal distribution at the false-alarm probability P_{fa}, $\rho = N^{\mathrm{inv}}(0, 1, P_{\mathrm{fa}})$, as follows ([3]):

$$P_{\mathrm{res},\mu} = \mathbb{P}\{\xi_{\mathrm{LR},\boldsymbol{\mu}(\theta)} > \rho \mid H_1\}, \ \xi_{\mathrm{LR},\boldsymbol{\mu}(\theta)} \sim N(d_{\boldsymbol{\mu}(\theta)}, 1) \ . \quad (12)$$

In cases with Gaussian data as in (1)-(4), other information (pseudo-)distances can also be used to compute the test statistic $\xi_{\mathrm{LR},\boldsymbol{\mu}(\theta)}$ of the resolution bound $P_{\mathrm{res},\mu}$. For example, the Kullback-Leibler divergence d_{KL} and Bhattacharyya distance d_{BT}, are related to the information distance $d_{\boldsymbol{\mu}(\theta)}$ (and also to LR, [3]) as: $d_{\mathrm{KL}} = \mathrm{E}_{H_1}[\ln \mathrm{LR}] = d^2_{\boldsymbol{\mu}(\theta)}$ and $d_{\mathrm{BT}} = -\ln \mathrm{E}_{H_0}\left[\sqrt{\mathrm{LR}}\right] = d^2_{\boldsymbol{\mu}(\theta)}/4$, respectively.

With the measurements from NS, SS and RM, the stochastic resolution bounds $P_{\mathrm{res},\mu,\mathrm{NS}}$, $P_{\mathrm{res},\mu,\mathrm{SS}}$ and $P_{\mathrm{res},\mu,\mathrm{RM}}$ are computed from (12) by using the distances $d_{\boldsymbol{\mu}(\theta),\mathrm{NS}}$, $d_{\boldsymbol{\mu}(\theta),\mathrm{SS}}$ and $d_{\boldsymbol{\mu}(\theta),\mathrm{RM}}$ from (7), (8) and (9), respectively.

Finally, the resolution bounds given by the IG-based probability $P_{\mathrm{res},\mu}$ in (12) are compared with the SSP resolution whose probability $P_{\mathrm{res,SSP}}$ is assessed numerically from $\boldsymbol{x}_{\mathrm{SSP}}$ in (5) for the two target cells i and j, $i \neq j$, by:

$$P_{\mathrm{res,SSP}} = \mathbb{P}\{(x_{\mathrm{SSP},i} \neq 0) \wedge (x_{\mathrm{SSP},j} \neq 0) | H_1\} \quad (13)$$

where SSP in (5) uses η given by: $\eta^2 = -\gamma \ln P_{\mathrm{fa}}$ (e.g. [24]). In NS, SS and RM, the SSP resolution probabilities $P_{\mathrm{res,SSP,NS}}$, $P_{\mathrm{res,SSP,SS}}$ and $P_{\mathrm{res,SSP,RM}}$ are assessed with the SSP estimates from (5) obtained with the measurements modelled in (2), (3) and (4), respectively.

IV. Numerical Results

The resolution analysis from Section III is demonstrated with numerical tests from array processing of two close equal targets at different SNRs. The measurements $\boldsymbol{y}$ from (1) are acquired from a linear array of size N, and contain responses from two point-targets separated by $\delta\theta$, $\boldsymbol{y} = \boldsymbol{\mu}(\theta) + \boldsymbol{\mu}(\theta + \delta\theta) + \boldsymbol{z}$. The total number N of array elements is chosen to be 100 while a number M of compressive measurements is chosen to be 50 and 25, i.e. the compression factor N/M equals 2 and 4, respectively. The observation grid is Nyquist in NS as $N = M$, or sub-Nyquist in SS and RM as $N > M$. The mn–th element: $\exp(j\varphi_{mn})/\sqrt{M}$, of the random matrix $\boldsymbol{B}_{\mathrm{RM}}$ represents a phase shift by a uniformly-distributed angle φ_{mn}, $\varphi_{mn} \sim U(0,2\pi)$. A multi-coset pattern is chosen for $\boldsymbol{B}_{\mathrm{SS}}$ whose array edge elements are always kept equal to one (so that the array size D_β remains the same).

The true input signal s is kept the same in all the acquisition schemes. The estimation grid of size N is also kept the same. The targets are separated in θ by δθ up to three Nyquist cells large, i.e. up to $6\pi/N$. The signal amplitude $|s|$ equals $\sqrt{\gamma\text{SNR}}$ and the noise variance γ is constant, γ =1. The false-alarm probability P_{fa} is set to 0.000001 (as realistic in radar) in ρ and η from (12) and (13).

In Fig. 1, the information distances $d_{\boldsymbol{\mu}(\theta),\text{NS}}$, $d_{\boldsymbol{\mu}(\theta),\text{SS}}$ and $d_{\boldsymbol{\mu}(\theta),\text{RM}}$ computed from (7), (8) and (9), respectively, are also assessed numerically from the simulated data as the mean values from 100 Monte-Carlo realizations of the noise $\boldsymbol{z}$, and of the compression matrices $\boldsymbol{B}_{\text{SS}}$ and $\boldsymbol{B}_{\text{RM}}$. The analytical and numerical results of the information distances (normalized by $\sqrt{N}$ for the sake of clearer comparison) coincide.

In Fig. 2, the resolution bounds $P_{\text{res},\mu,\text{NS}}$, $P_{\text{res},\mu,\text{SS}}$ and $P_{\text{res},\mu,\text{RM}}$ together with the SSP probabilities $P_{\text{res,SSP,NS}}$, $P_{\text{res,SSP,SS}}$ and $P_{\text{res,SSP,RM}}$ are shown for the same 100 realizations of the test cases at δθ equal to $2\pi/N$ or $4\pi/N$. The bounds $P_{\text{res},\boldsymbol{\mu}_*}$ are far from $P_{\text{res,SSP},*}$, especially of SS. The resolution probabilities from RM and NS are comparable. In addition, at larger δθ (Fig. 2, bottom), $P_{\text{res},\boldsymbol{\mu}_*}$ and $P_{\text{res,SSP},*}$ remain nearly the same. This behavior agrees with the related information distance $d_{\boldsymbol{\mu}(\theta)}$ in Fig. 1 which also remains nearly the same at the larger separation.

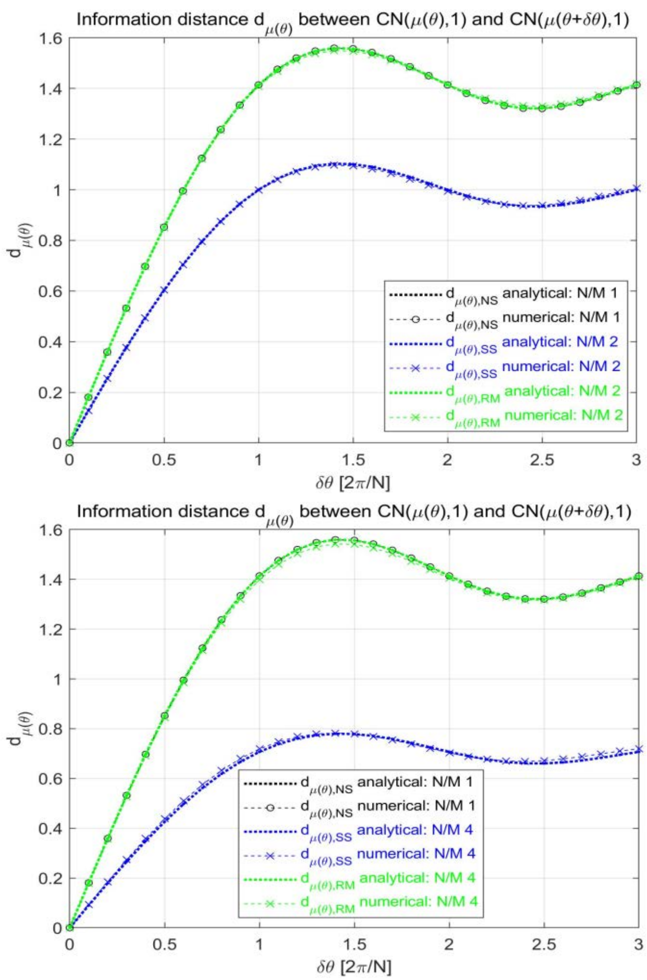

Fig. 1. Information distances from data acquisition schemes NS, SS and RM: $d_{\boldsymbol{\mu}(\theta),\text{NS}}$, $d_{\boldsymbol{\mu}(\theta),\text{SS}}$ and $d_{\boldsymbol{\mu}(\theta),\text{RM}}$ versus separation δθ at unit SNR and compression factor M/N equal to 2 (top) and 4 (bottom) in SS and RM, computed from (7), (8) and (9), respectively, and assessed numerically as the average values from 100 Monte-Carlo runs.

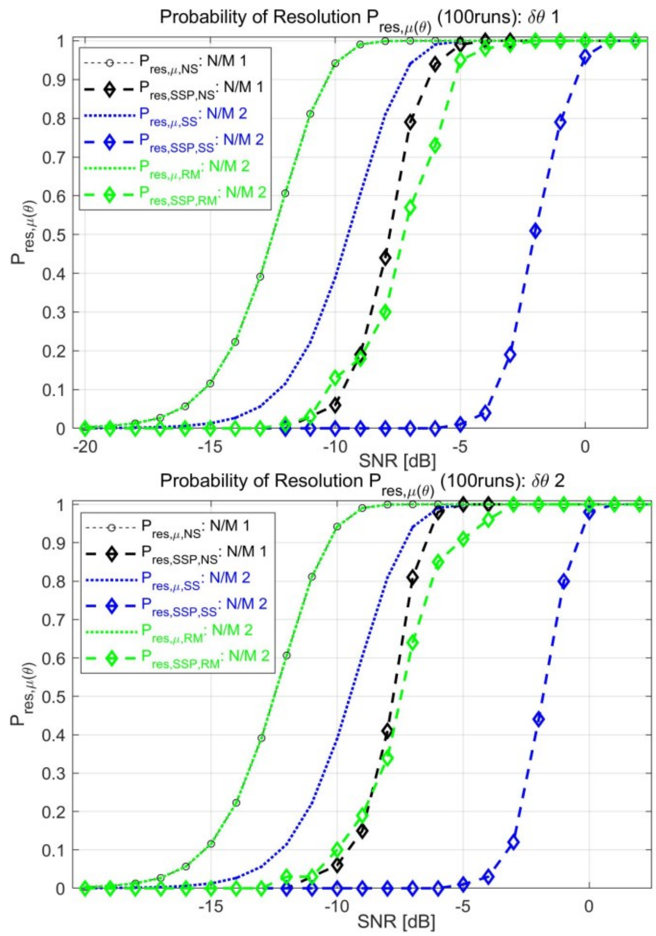

Fig. 2. Resolution of data acquisition schemes NS, SS and RM given by the resolution bounds computed from (12): $P_{\text{res},\mu,\text{NS}}$, $P_{\text{res},\mu,\text{SS}}$ and $P_{\text{res},\mu,\text{RM}}$, together with the related SSP resolution probabilities obtained from (13): $P_{\text{res,SSP,NS}}$, $P_{\text{res,SSP,SS}}$ and $P_{\text{res,SSP,RM}}$, respectively, at separation δθ equal to one (top) and two (bottom) Nyquist cells and compression N/M equal to 2 in SS and RM. Test cases as in Fig. 1.

V. CONCLUSIONS

The resolution performance of typical sub-Nyquist data acquisition schemes from CS was assessed, and moreover, compared with the performance of the corresponding Nyquist-sampled scheme as the reference.

The resolution analysis demonstrated that a CS sensor can be simpler with fewer measurements and can still perform as good as existing sensors. This is true only in the case of compressive data acquisition starting directly at reception with no receiver noise yet, and thus, affecting the signal only. An example of the scheme is random masking.

In future work, the performance of CS radar is being further assessed by evaluating the SSP detection and accuracy when compressive data acquisition is applied. Furthermore, the continuous domain is being analyzed to determine the reference (before any sampling) for the performance analysis of compressive measurements.

REFERENCES

[1] D. Donoho, “Compressed sensing,” *IEEE Trans. on IT* 52/4, 2005.

[2] P. Pakrooh, L. L. Scharf, A. Pezeshki, and Y. Chi, “*Analysis of Fisher information and the Cramer-Rao bound for nonlinear parameter estimation after compressed sensing*”, IEEE Conference ICASSP 2013.

[3] R.Pribić and G.Leus, “*Information Distances for Radar Resolution Analysis*”, in Special Session on “Information Geometry in Signal Processing” at IEEE Workshop CAMSAP 2017.

[4] C.Tzotzadinis, “*Performance and Complexity of Data Acquisition in CS Radar*”, TU Delft MSc Thesis at Thales NL, December 2017.

[5] R. Pribic, G.Leus and C.Tzotzadinis, “*Signal-to-Noise Ratio Analysis of Compressive Data Acquisition*”, Special Session on “Sparsity in Estimation” at IEEE Workshop SSP 2018.

[6] A. J. den Dekker and A. van den Bos, “Resolution: a survey", *J. of the Opt. Soc. of America A*, 14/3, 1997.

[7] S. T. Smith, “Statistical resolution limits and the complexified CR bounds”, *IEEE Trans. on SP* 53/5, 2005.

[8] Zhi Liu and A. Nehorai, “Statistical angular resolution limit for point sources”, *IEEE Trans. on SP* 55/11, 2007.

[9] Y. Cheng, X. Wang, T. Caelli, X. Li and B. Moran, “On information resolution of radar systems", *IEEE Trans on AES* 48/4, 2012.

[10] C. R. Rao. Information and the accuracy attainable in the estimation of statistical parameters. Bull. Calcutta Math.Soc. 37, pp. 81-89, 1945.

[11] S. Amari. "Information geometry of statistical inference - an overview", *IEEE* IT Workshop, 2002.

[12] E. Candès and C. Fernandez-Granda, “Towards a Mathematical Theory of Super-resolution”, Willey Communications on Pure and Aplied Mathematics, vol.67/no.7, 2014.

[13] G. Schiebinger, E. Robeva and B. Recht, “Superresolution without Separation”, *IEEE* CAMSAP 2015.

[14] E. de Jong and R. Pribić, “Sparse signal processing on estimation grid with constant information distance applied in radar”, *EURASIP Journal on Advances in SP,* 2014:78.

[15] M. Coutino, R. Pribić and G. Leus, “Direction of arrival estimation based on information geometry”, *IEEE* ICASSP 2016.

[16] R. Pribić, M. Coutino and G. Leus, “Stochastic Resolution Analysis of Co-prime Arrays in Radar”, *IEEE* SSP 2016.

[17] R. Pribić, “Stochastic Resolution Analysis via a GLR Test in Radar”, *IEEE* CoSeRa 2016.

[18] H. L. Van Trees. *Optimum Array Processing*. Wiley, 2002.

[19] C. E. Cook and M. Bernfeld. *Radar signals; an introduction to theory and application.* Acad.Press, 1967.

[20] Y. Kochman and G. W. Wornell, “*Finite Multi-coset Sampling and Sparse Arrays*,” Information Theory and Applications Workshop (ITA). IEEE, 2011.

[21] R. Tibshirani, “Regression Shrinkage and Selection via the Lasso”, J. of R. Stat. Soc, Series B, Vol. 58/issue 1, 1996.

[22] J. L. Strapasson, J. Pinele and S.I.R. Costa, "A Totally Geodesic Submanifold of the Multivariate Normal Distributions and Bounds for the Fisher-Rao Distance," IEEE ITW 2016.

[23] S.M Kay. *Fundamentals of Statistical Signal Processing Vol. II: Estimation Theory*. Prentice Hall, 1998

[24] J.J. Fuchs, “The GLRT and the Sparse Representations Approach”, vol. 6134, pp. 245–253, of *ICISP in Lecture Notes in Computer Science*. Springer Berlin Heidelberg, 2010.

[25] yall1: your algorithms for L1, http://yall1.blogs.rice.edu/.